




# Metabolomic Analysis Reveals that SPHK1 Promotes Oral Squamous Cell Carcinoma Progression through NF- $\kappa$ B Activation

Chen-xing Hou, MD<sup>1,2</sup>, Guang-yan Mao, MD<sup>1,3</sup>, Qiu-wangyue Sun, MD<sup>1,4</sup>, Ying Meng, MD<sup>1,2</sup>, Qing-hai Zhu, MD<sup>1,2</sup>, Yu-ting Tang, MD<sup>1,2</sup>, Wei Han, MD<sup>1,2</sup>, Nan-nan Sun, MD<sup>1,2</sup>, Xiao-meng Song, MD, PhD<sup>1,2</sup>, Chen-xing Wang, MD, PhD<sup>1,2</sup>, and Jin-hai Ye, MD, PhD<sup>1,2</sup> 

<sup>1</sup>Jiangsu Key Laboratory of Oral Disease, & Jiangsu Province Engineering Research Center of Stomatological Translational Medicine, Nanjing Medical University, Nanjing, China; <sup>2</sup>Department of Oral and Maxillofacial Surgery, The Affiliated Stomatological Hospital of Nanjing Medical University, Nanjing, China; <sup>3</sup>Department of Stomatology, School of Medicine, Nanjing Tongren Hospital, Southeast University, Nanjing, China; <sup>4</sup>Department of Stomatology, Affiliated Huaian Number 1 People's Hospital of Nanjing Medical University, Huai'an, China

## ABSTRACT

**Background.** Metabolic disorders are significant in the occurrence and development of malignant tumors. Changes of specific metabolites and metabolic pathways are molecular therapeutic targets. This study aims to determine the metabolic differences between oral squamous cell carcinoma (OSCC) tissues and paired adjacent non-cancerous tissues (ANT) through liquid chromatography-mass spectrometry (LC-MS). SPHK1 is a key enzyme in sphingolipid metabolism. This study also investigates the potential role of SPHK1 in OSCC.

**Materials and Methods.** This study used LC-MS to analyze metabolic differences between OSCC tissues and paired ANT. Principal component analysis (PCA) and partial least-squares discriminant analysis (PLS-DA) were applied to explain the significance of phospholipid metabolism pathways in the occurrence and development of OSCC. Through further experiments, we confirmed the

oncogenic phenotypes of SPHK1 in vitro and in vivo, including proliferation, migration, and invasion.

**Results.** The sphingolipid metabolic pathway was significantly activated in OSCC, and the key enzyme SPHK1 was significantly upregulated in oral cancer tissues, predicting poor OSCC prognosis. In this study, SPHK1 overexpression was associated with high-grade malignancy and poor OSCC prognosis. SPHK1 targeted NF- $\kappa$ B by facilitating p65 expression to regulate OSCC tumor progression and promote metastasis.

**Conclusions.** This study identified metabolic differences between OSCC and paired ANT, explored the carcinogenic role of overexpressed SPHK1, and revealed the association of SPHK1 with poor OSCC prognosis. SPHK1 targets NF- $\kappa$ B signaling by facilitating p65 expression to regulate tumor progression and promote tumor metastasis, providing potential therapeutic targets for diagnosing and treating oral tumors.

---

Chen-xing Hou, Guang-yan Mao and Qiu-wangyue Sun contributed equally to this work.

---

© Society of Surgical Oncology 2022

First Received: 7 February 2022

Accepted: 16 June 2022

Published Online: 12 July 2022

C. Wang, MD, PhD

e-mail: doctorwxc@njmu.edu.cn

J. Ye, MD, PhD

e-mail: yejinhai@njmu.edu.cn; yjh98001@163.com

Oral squamous cell carcinoma (OSCC) constitutes 90% of oral cancers, the sixth most commonly diagnosed cancer. OSCC originates from the squamous epithelium lining, accounting for 2–4% of all malignant tumors in the body.<sup>1–3</sup> Alone, oral and oropharyngeal cancer affects 6 per 100,000 individuals, a relatively high incidence rate, in Western countries.<sup>4</sup> During the past two decades, the incidence rate of oral cancer has increased sharply, and the 5-year survival rate for patients is only 50%.<sup>5</sup> Treatment includes surgical resection, chemotherapy, and radiotherapy, but the therapeutic effect in oral cancer remains

unsatisfactory.<sup>6</sup> Therefore, the discovery of genes related to oral cancer and understanding the mechanism of disease development are important for finding effective therapeutic targets to improve the survival and prognosis of patients with OSCC.

Metabolomics, a newly emerging branch of systems biology, qualitatively and quantitatively analyzes metabolites and metabolic pathways in organisms. Metabolic disorders are significant in the occurrence and development of malignant tumors. Changes of specific metabolites and metabolic pathways are potential cancer markers (PCMs). Recently, nuclear magnetic resonance (NMR) spectroscopy and mass spectrometry (MS) techniques have increasingly been integrated to assess tumor phenotypes in metabolomics research. Current OSCC metabolomics research mainly involves cell lines and body fluids,<sup>7</sup> including plasma,<sup>8</sup> serum,<sup>9</sup> urine,<sup>10</sup> and saliva.<sup>11,12</sup> However, metabolomics analysis of tumor tissue mostly involves NMR spectroscopy technology.<sup>13</sup>

This study uses ultraperformance liquid chromatography time-of-flight mass spectrometry (UPLC-TOF-MS) to analyze OSCC and adjacent noncancerous tissues (ANT). The aim of this work is to improve the clinical sample collection process, establish a sample bank containing complete clinical and pathological parameters and follow-up information, and optimize the pretreatment conditions and liquid chromatography-mass spectrometry (LC-MS) conditions of tissue samples. Principal component analysis (PCA) and partial least-squares discriminant analysis (PLS-DA) explained the significance of different metabolites and metabolic pathways in the occurrence and development of OSCC.

In cellular metabolic processes, sphingolipids are ubiquitous components of mammalian cell membranes, necessary for regulating many disease-related cellular processes. Ceramide and sphingosine inhibit cell proliferation and induce apoptosis, while the metabolite, sphingosine-1-phosphate, promotes cell proliferation and inhibits apoptosis.<sup>14,15</sup> Sphingosine kinase (SPHK), a key enzyme in sphingolipid metabolism, converts sphingosine to sphingosine-1-phosphate, important in physiological equilibrium. SPHK is a highly conserved lipid kinase with two isoenzyme structures: SPHK1 and SPHK2. The wild-type *SPHK1* gene was first identified as an oncogene in 2000.<sup>16</sup> Subsequently, SPHK1 was found to be significantly increased in malignant tumors including lung,<sup>17</sup> gastric,<sup>18</sup> liver,<sup>19,20</sup> breast,<sup>21</sup> and colorectal cancers.<sup>22</sup> Although these studies indicate SPHK1 as a potential carcinogen in various cancers, the specific carcinogenic mechanism of SPHK1 is obscure. The role and mechanism of SPHK1 in oral cancer tumorigenesis and development remain unclear.

This study aims to determine the metabolic differences between OSCC and paired adjacent noncancerous tissue through LC-MS. The study also sets out to investigate the potential role of SPHK1 in OSCC cells and describe the influence of SPHK1 on p65 expression via direct NF- $\kappa$ B targeting, which would be crucial in affecting the subsequent promotion of malignant phenotype progression.

## MATERIALS AND METHODS

### *Patients and Samples*

The included patients were those admitted for surgery from September 2015 to July 2017 at the Department of Oral and Maxillofacial Surgery at the Affiliated Stomatological Hospital of Nanjing Medical University, Jiangsu Province, China. The inclusion and exclusion criteria for participants and sample collection procedures were as follows: participants involved in this study were not taking any medications, and those suffering from metabolic diseases, liver diseases, kidney diseases, or any other types of cancer were excluded.

Eighteen pairs of fresh OSCC and normal adjacent tissue from patients receiving radical oral cancer operation at the Affiliated Stomatological Hospital of Nanjing Medical University were assessed using quantitative real-time polymerase chain reaction (qRT-PCR). Twelve pairs of OSCC and normal adjacent tissue samples were evaluated using western blot assay, and 15 pairs of OSCC and normal adjacent tissue samples were assessed using UPLC-TOF-MS. Fifty-four OSCC excised lesions were evaluated using immunohistochemistry (IHC) and prognosis analysis. All patients provided written informed consent. Each patient provided clinical, pathological, and follow-up data. The Research Ethics Committee of Nanjing Medical University reviewed and approved this study.

### *Chromatography*

A 2- $\mu$ l aliquot of the pretreated sample was injected into an Agilent InfinityLab Poroshell 120 column (Agilent Technologies, CA) on an Agilent 1260 Infinity II liquid chromatography system (Agilent Technologies, CA). The mobile phase consisted of 0.1% (v/v) formic acid (solvent A) and 100% (v/v) acetonitrile (solvent B). The flow rate was 0.4 ml/min with a column temperature of 35°C. The gradient conditions were: 0–2 min: 5% B; 2.0–2.5 min: 20% B; 2.5–6.0 min: 45% B; 6.0–7.5 min: 90% B; 7.5–8.0 min: 92.5% B; 8.0–12.0 min: 97.5% B; and after 12.0 min, it increased to 100% B. After each analytical run, the mobile phase was equilibrated at 5% B for 3 min. All samples were randomly analyzed in succession to

minimize the analytical variation. Additionally, quality control (QC) samples were analyzed at the beginning and end of each batch run to ensure stability during analysis.

### Mass Spectrometry

Data acquisition was performed with an Agilent 6530 Q-TOF mass spectrometry system (Agilent Technologies, CA) equipped with an electrospray ionization source operating in ESI<sup>-</sup> mode. The capillary voltage was 3.0 kV. The dry gas was nitrogen, and the desolvation gas flow was 10 L/min at 350 °C desolvation temperature. Data were collected in full scan mode from 50 to 1000 *m/z*.

### Cell Culture and Construction of Stable Cell Lines

Cal 27, HN4, and HN6 OSCC cell lines were purchased from the American Type Culture Collection (ATCC, VA) and cultured at 37 °C in a gas containing 5% CO<sub>2</sub>. The cells were cultured in DMEM containing 10% fetal bovine serum (Gibco, MA). Genechem Co. Ltd (Shanghai, China) designed and constructed the lentivirus vector. The SPHK1 shRNA (shSPHK1) and control short hairpin RNA (shNC) were transfected into Cal 27 cells to produce SPHK1 knockdown cells following the manufacturer's instructions.

### CCK8 and Colony Formation Assay

For CCK8 assays, shSPHK1 Cal 27 cells (1000 cells per well) were cultured in a 96-well plate. The CCK8 assay determined the OD value of shSPHK1 Cal 27 cells at 450 nm wavelength for three consecutive days. For the colony formation assays, 3000 cells were seeded in each well in a six-well plate. After 2 weeks of incubation, cells were stained with 0.1% crystal violet.

### Cell Migration and Invasion Assay

Cells were cultured to 80–90% confluence in a six-well plate and marked with a 100 UL gun head. Marked cells were cultured for 24 h without serum starvation. Images were taken at 0 and 24 h to evaluate the wound healing ability. The transwell chamber with 8 μm pore diameter was used to measure the invasion and migration ability of the cells. For the migration assay, 2 × 10<sup>5</sup> cells were seeded into the upper transwell chamber under serum-free conditions. For the invasion assay, glue was diluted at a 1:20 ratio and placed at the bottom of the chamber, while 5 × 10<sup>6</sup> cells were placed in the upper compartment under starvation. The lower part of the chamber was 800 μl Dulbecco's modified Eagle medium (DMEM) with 10%

fetal bovine serum (FBS). After incubation for 48 h, cells were stained using 0.1% crystal violet.

### Western Blot Analysis

Cells or tissues were lysed with radioimmunoprecipitation assay (RIPA) solution, and proteins with different molecular weights were separated with 8–12% sodium dodecyl sulfate-polyacrylamide gel electrophoresis (SDS-PAGE) gel and transferred to the polyvinylidene difluoride (PVDF) membrane. The membrane was incubated with the corresponding primary antibody at 4 °C overnight, washed thrice for 5 min each time, and coincubated with horseradish peroxidase (HRP)-labeled secondary antibody for 1 h. The membranes were again washed thrice and developed with the enhanced chemiluminescence (ECL) developer solution. The western blot antibodies included GAPDH (number 10494-1-AP), p65 (number 66535-1-Ig), and SPHK1 (number 10670-1-AP), from Proteintech (Chicago, IL), and p-p65 (number 3033) from Cell Signaling Technology (MA).

### Quantitative Real-Time PCR (qRT-PCR)

Total ribonucleic acid (RNA) was extracted from cells or tissues using TRIzol (Thermo Fisher Scientific, MA) and reverse-transcribed to cDNA using PrimeScript RT Master Mix (Takara Bio Inc, Kusatsu-Shiga, Japan). PCR amplification was performed using Takara TB Green Premix Ex Taq II (Tli RNaseH Plus) (Takara Bio Inc, Kusatsu-Shiga, Japan). The internal reference and primer sequences were obtained from Nanjing Kingsley Company and are presented in Table 1.

### Immunohistochemistry (IHC)

Slides were stained using the MaxVision TM2 Kit (MXB Biotechnologies, Fujian, China) following the manufacturer's instructions. The positive intensity of immunohistochemistry was divided into five grades according to the proportion of positive cells: 0, < 5%; 1, 6–25%; 2, 26–50%; 3, 51–75%; and 4, > 75%, choosing at least three microscopic fields of view (20×). Grades 0–2

**TABLE 1** Primer sequences for qRT-PCR

GAPDH-FP	5'-CATCTCTGCCCCCTCTGCTGA-3'
GAPDH-RP	5'-GGATGACCTTGCCACAGCCT-3'
Sphk1-F	5'-TGGCCTACCTCCCTGTAGGA-3'
Sphk1-R	5'-CATGGGTGCAGCAAACATCT-3'

are lower expression, and grades 3–4 are higher expression. Two experienced pathologists evaluated the results. The primary antibodies were SPHK1 (number 10670-1-AP), Ki67 (number 27309-1-AP), E-cadherin (number 20874-1-AP), and vimentin (number 10366-1-AP) from Proteintech (Chicago, IL).

#### *In Vivo Subcutaneous Xenograft Models*

Nude mice were obtained from the Experimental Animal Center of Nanjing Medical University (Nanjing, China). The Ethical Review Committee of the Experimental Animal Welfare of Nanjing Medical University (Nanjing, China) approved the experiment. Nude mice were raised in the Experimental Animal Experimental Center of Nanjing Medical University. The stably transfected SPHK1 knockdown and control cells ( $5 \times 10^7$ ) were resuspended in 200  $\mu$ l DMEM. Then, we injected DMEM with cells into the left abdomen of BALB/C nude mice (female; 6 weeks of age). The tumor volume and weight were measured every 7 days. At 42 days after injection, the nude mice were sacrificed, and tumors were collected. One part of the tumor was fixed in formalin for immunohistochemistry, and the other was frozen for western blot analysis.

#### *Statistical Analysis*

For the untargeted metabolomics analysis, PCA was used to determine the stability and replication detection. Partial least-squares discriminant analysis (PLS-DA) was applied to evaluate the differences between sample groups, and MATLAB software was used to identify outliers. Variable important in projection (VIP) values were calculated for each variable. Potential biomarkers were selected on the basis of  $P$  and VIP values. Each experiment was independently repeated three times, and the results were presented as mean  $\pm$  standard deviation.  $P < 0.05$  indicated statistically significant difference. The Kaplan–Meier analysis assessed the overall survival differences. All statistical analyses were performed using GraphPad Prism or ImageJ software.

## RESULTS

### *Phospholipid Metabolism Was Significantly Abnormal in OSCC Tissues*

Abnormal metabolism is a significant feature in malignant tumor development. Fifteen pairs of matched oral squamous cell carcinoma tissues (OSCC) and adjacent noncancerous tissues (ANT) were collected for nontargeted

metabolomics analysis to study the difference between metabolite and metabolic pathways in OSCC. After excluding isotopic peaks, there were 656 metabolic profiling ions (peaks) in the negative electrospray ionization (ESI<sup>-</sup>) mode, of which 374 ions ( $P < 0.05$ ) were used for further analysis.

PCA of 30 samples revealed that both sample groups were tightly clustered, indicating the high quality of the metabolic profiling platform (Fig. 1a). The PLS-DA score plot indicated that OSCC and adjacent noncancerous tissues had different metabolic profiles (Fig. 1b). On the basis of the two criteria of  $P < 0.05$  and  $VIP > 0.30$ , 148 differentially expressed metabolites were identified for further pathway analysis (Fig. 1c). At  $P < 0.05$  and  $VIP > 0.70$ , 16 differentially expressed metabolites were identified (Table 2). Their concentration variations are shown as box plots in Fig. 1d. Among these metabolites, 3-hydroxytamoxifen, 4-nitrophenol, deoxycytidine, 5 $\alpha$ -tetrahydrocortisol, 11-dehydrocorticosterone, and debrisoquine were considered exogenous drug-related metabolites. Receiver operating characteristic (ROC) curve analysis was performed on four endogenous differential metabolites within  $P < 0.05$  and  $VIP > 1$ . The area under curve (AUC) values for citrulline, lysophosphatidylcholine, and dodecanedioylcarnitine were greater than 0.9, a high diagnostic value (Fig. 1e). All metabolites were identified on the basis of the original mass spectrum data and the Human Metabolome Database.

A metabolic set enrichment analysis (MSEA) using the MetaboAnalyst database on the 148 differential ions (less exogenous substances) identified and visualized the differences in metabolic pathways between OSCC and ANT (Fig. 1f). The path analysis using the MetaboAnalyst database leveraged the  $m/z$  features and metabolic network by mapping the possible metabolites on the pathways in one step. Sphingolipid was the most significantly affected metabolic pathway ( $P \leq 0.05$ ), followed by arginine and proline (Fig. 1g).

### *SPHK1 Was Significantly Upregulated and Associated with Poor Prognosis in OSCC Patients*

SPHK1 is the key enzyme of sphingolipid metabolism in OSCC. Gene Expression Profiling Interactive Analysis (GEPIA) online database analysis of SPHK1 expression in normal and head and neck squamous cell carcinoma (HNSCC) patients [data from The Cancer Genome Atlas (TCGA) database] showed that SPHK1 was significantly upregulated in HNSCC patients (Fig. 2a). Real-time quantitative PCR analysis of *SPHK1* mRNA expression in 18 pairs of OSCC and adjacent normal tissues showed that *SPHK1* mRNA levels significantly increased in OSCC tissues (Fig. 2b). As with mRNA, the SPHK1 protein levels

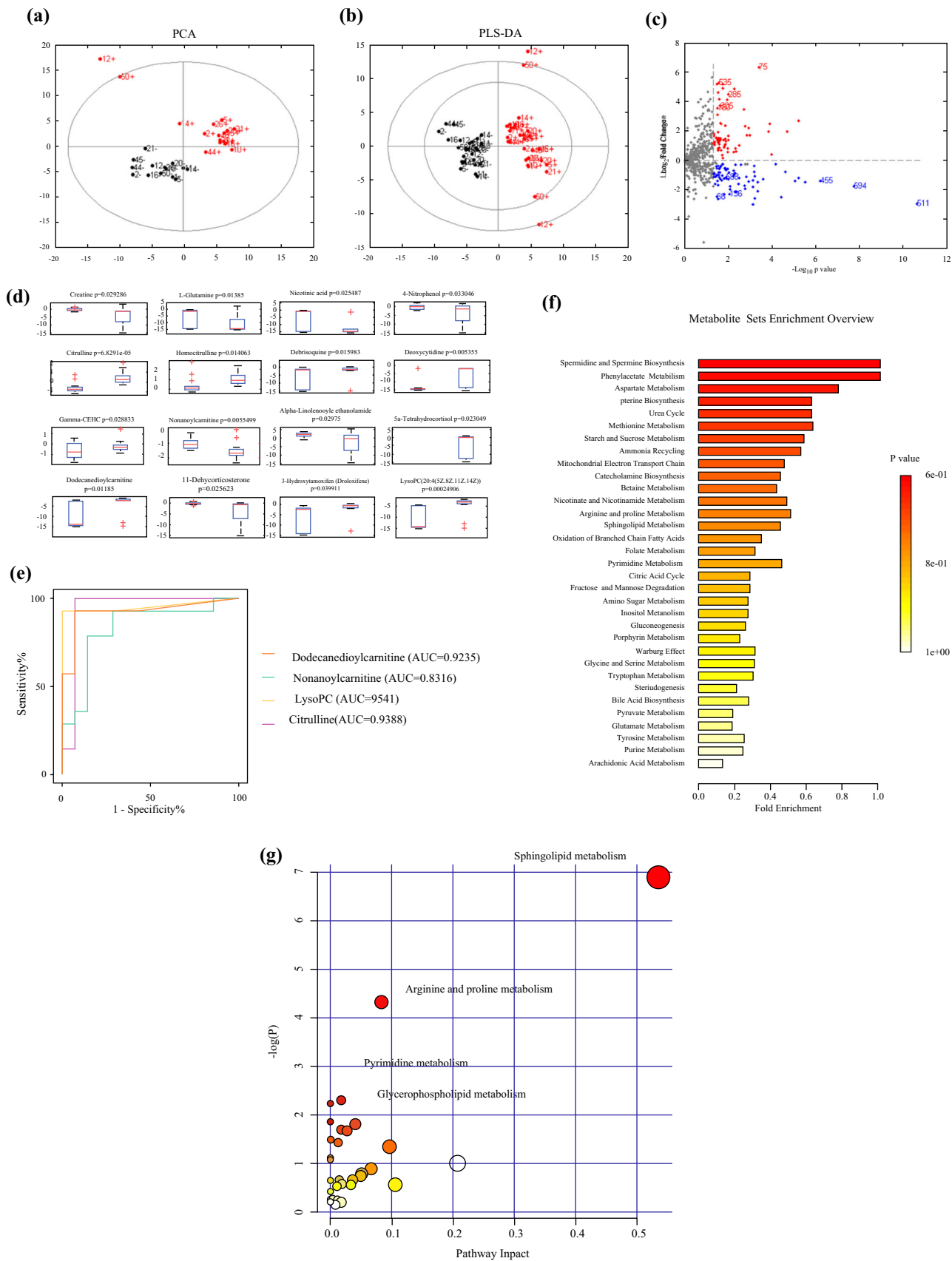




**FIG. 1** Phospholipid metabolism was significantly abnormal in OSCC tissues; **a** PCA score plots for discriminating OSCCT and ANT, **b** PLS-DA for discriminating OSCCT and ANT, **c** volcano plots of ion variations, **d** box plots showing the concentration variations of metabolites, **e** ROC curves of typical metabolite variations, **f** results showing metabolite variations from metabolite set enrichment analysis, and **g** pathway impact map constructed by MetaboAnalyst database

were significantly higher in OSCC than in normal tissues according to western blot and immunohistochemistry analyses (Fig. 2c, d). The IHC results also showed that SPHK1 expression correlated with clinical stage (Fig. 2e; Supplementary Fig. 1A).

Further investigation showed a correlation between SPHK1 expression and the clinical prognosis of patients. We analyzed the OSCC tissues of patients undergoing radical OSCC surgery in our hospital and divided them into two groups by SPHK1 immunohistochemical score. The 54 samples with visible SPHK1 staining on IHC and complete follow-up data analyzed by Kaplan–Meier survival analysis showed high SPHK1 expression and predicted low overall survival (Fig. 2f; Table 3).

#### *SPHK1 Promoted Cell Proliferation and Inhibited Apoptosis in OSCC Cells*

Considering the differential expression of SPHK1 in clinical samples, the expression and function of SPHK1 in

OSCC cells were further evaluated. Western blot assay was used to determine SPHK1 expression in normal squamous epithelial cells and squamous cell carcinoma cells of the oral cavity (Fig. 3a). The SPHK1-targeting shRNA (shSPHK1) or corresponding controls (shNC) established the stable SPHK1-knockdown cell lines in Cal 27 cells with highly endogenous SPHK1 expression. Besides, SPHK1-expressing recombinant lentivirus (Lv-SPHK1) and control vectors (Lv-NC) were also introduced into HN6 cells to establish the stable SPHK1 overexpressed cell lines. Western blot analysis was conducted to confirm the transfection efficiency (Fig. 3b). The study showed that SPHK1 knockdown significantly reduced the proliferation and colony formation of Cal 27 cells, while SPHK1 overexpression can promote proliferation and colony formation in HN6 cells (Fig. 3c, d). Further western blot analysis and terminal deoxynucleotidyl transferase dUTP nick end labeling (TUNEL) staining established that SPHK1 could promote cell proliferation and inhibited apoptosis in both Cal 27 and HN6 cell lines (Fig. 3e, f; Supplementary Fig. 1b, c). In conclusion, these results showed the oncogenic role of SPHK1 in proliferating and inhibiting apoptosis in Cal 27 and HN6 cells in vitro.

#### *SPHK1 Enhances Epithelial–Mesenchymal Transformation (EMT) in OSCC Cell Lines*

The migration and invasion ability of Cal 27 and HN6 cells were measured with wound healing and transwell

**TABLE 2** Typical metabolite variations between OSCCT and ANT

Sequence number	Retention time (s)	Mass to charge ratio ( <i>m/z</i> )	Molecular formula	Metabolite	VIP	<i>P</i> value	Trend
1	212.69994	174.0957	C6H13N3O3	Citrulline	1.48	0.0001	↑
2	592.56006	578.2961	C28H50NO7P	Lysophosphatidylcholine	1.36	0.0002	↓
3	467.159898	300.2175	C16H31NO4	Nonanoylcarnitine	1.09	0.0055	↓
4	147.000018	262.0556	C9H13N3O4	Deoxycytidine	1.09	0.0054	↓
5	535.43988	372.2406	C19H35NO6	Dodecanedioylcarnitine	1.03	0.0119	↓
6	220.740036	188.1101	C7H15N3O3	Homocitrulline	0.98	0.0141	↓
7	227.57997	145.0609	C5H10N2O3	L-Glutamine	0.98	0.0138	↓
8	382.800036	283.1185	C15H20O3	gamma-carboxyethyl hydroxychroman	0.93	0.0288	↓
9	548.75982	365.2359	C21H34O5	5a-Tetrahydrocortisol	0.91	0.0230	↑
10	125.879988	158.0079	C6H5NO2	Nicotinic acid	0.90	0.0255	↓
11	624.48006	379.1765	C21H28O4	11-Dehydrocorticosterone	0.90	0.0256	↓
12	423.00012	320.25	C20H35NO2	Alpha-Linolenoyl ethanolamide	0.89	0.0297	↑
13	176.999988	130.0707	C4H9N3O2	Creatine	0.87	0.0293	↓
14	520.86	386.2112	C26H29NO2	3-Hydroxytamoxifen	0.87	0.0399	↓
15	200.520012	174.0061	C6H5NO3	4-Nitrophenol	0.86	0.0330	↓
16	220.740036	210.0902	C10H13N3	Debrisoquine	0.72	0.0160	↓

This table is sorted by VIP value; “Molecular formula” is from HMDB; ↑ means metabolites increased, and ↓ means metabolites decreased in the OSCC group

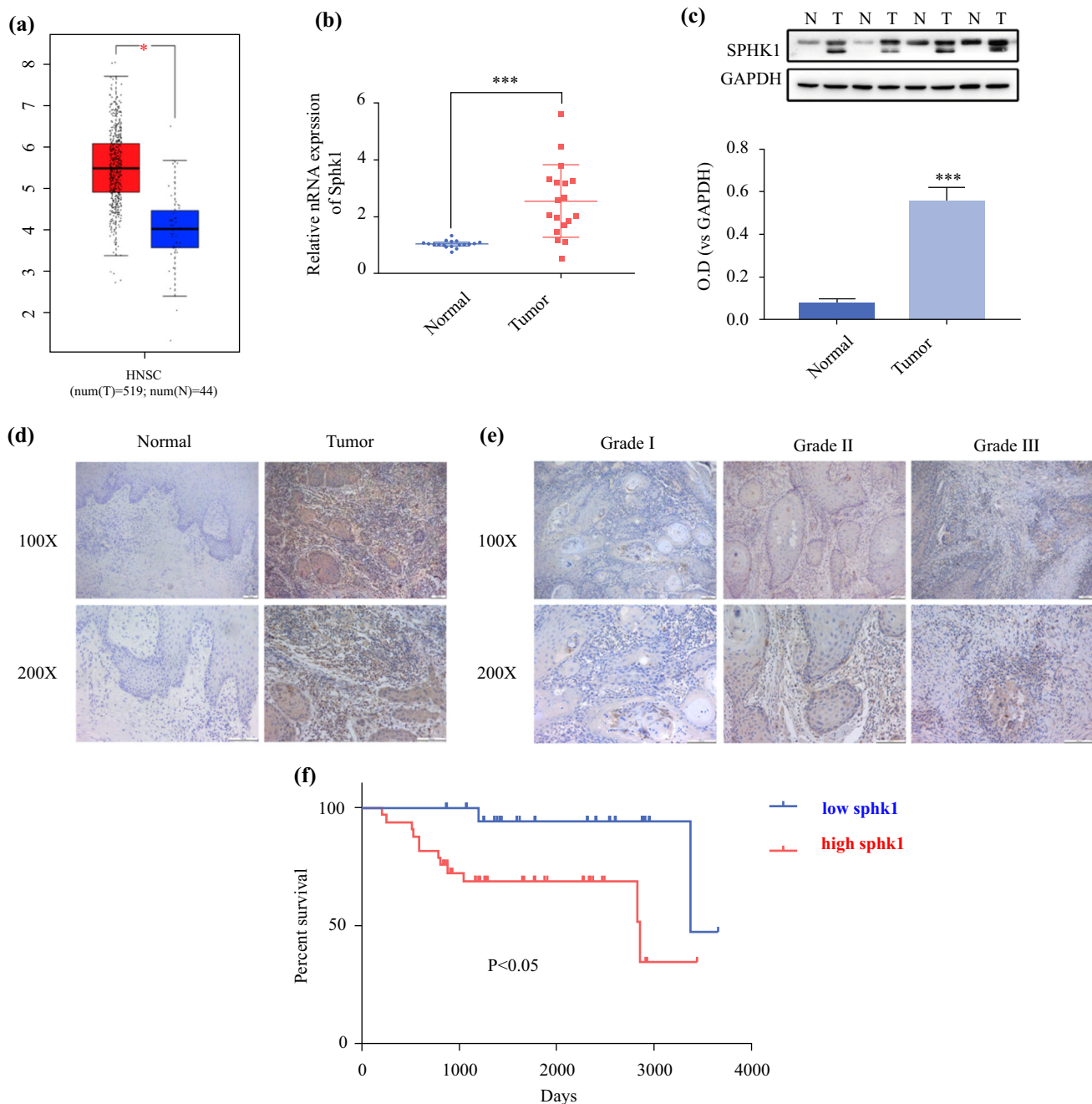


**FIG. 2** SPHK1 was significantly upregulated and predicted poor prognosis in OSCC patients; **a** SPHK1 expression in head and neck tissues from TCGA datasets, images were obtained from the GEPIA online database (<http://gepia.cancer-pku.cn>); **b** SPHK1 mRNA expression in 18 pairs of OSCC and adjacent normal tissues: results are shown as mean  $\pm$  SD. \* $P < 0.05$ , \*\* $P < 0.01$ , \*\*\* $P < 0.001$ , based on paired  $t$  tests; **c** western blot assay of SPHK1 protein expression in 12 pairs of OSCC and adjacent normal tissues measured

with GAPDH as the control, relative protein expression was measured by ImageJ and is shown as mean  $\pm$  SD. \* $P < 0.05$ , \*\* $P < 0.01$ , \*\*\* $P < 0.001$ , based on paired  $t$  tests; **d** SPHK1 immunohistochemical staining in OSCC and adjacent normal tissues; **e** SPHK1 expression correlated with the OSCC clinical stage; **f** overall survival rates of OSCC patients ( $n = 54$ ) according to SPHK1 expression

experiments. SPHK1 deletion in Cal 27 cells inhibited cell migration and invasion ability, and SPHK1 overexpression in HN6 cells promoted cell migration and invasion ability (Fig. 4a, b). Levels of EMT-related markers (E-cadherin,

vimentin, Slug, and ZO-1) were consistent with changes in SPHK1 (Fig. 4c, d), suggesting that SPHK1 could promote progression of EMT. Besides, immunofluorescence

**TABLE 3** Association between Sphk1 expression with clinicopathological parameters in 54 OSCC specimens

Clinicopathological parameters	Cases	Sphk1		P value
		Low	High	
Gender	54	20	34	
Male	28	11	17	$P > 0.05$
Female	26	9	17	
Age				
$\leq 60$ years	20	7	13	$P > 0.05$
$> 60$ years	34	13	21	
Tumor size				
T1–T2	36	17	19	$P < 0.05$
T3–T4	18	3	15	
Pathological grade				
I	35	17	18	$P < 0.05$
II–III	19	3	16	
Cervical node metastasis				
N (0)	35	14	21	$P > 0.05$
N (+)	19	6	13	

established that SPHK1 knockdown weakened the EMT process in cells (Supplementary Fig. 2).

#### SPHK1 Knockdown Inhibits Tumor Growth

Cal 27 cells with stably low SPHK1 expression (shSPHK1 groups) and control Cal 27 cells (NC groups) were inoculated into the left abdomen of nude mice to construct a xenograft tumor model of OSCC and explore the SPHK1 tumor-promoting effect in OSCC. The results showed that shSPHK1 groups had reduced tumor volumes and weights compared with NC groups (Fig. 5a, c). Additionally, shSPHK1 groups had significantly decreased SPHK1 and Ki67 expression (Fig. 5d) and EMT progression (Fig. 5e). Besides, TUNEL staining showed that shSPHK1 groups had increased apoptosis (Fig. 5f). Western blot analysis of shSPHK1 groups detected expression of proliferation, apoptosis, and EMT-related proteins similar to the *in vitro* results described above, where SPHK1 knockdown increased apoptosis and inhibited cell proliferation and EMT (Fig. 5g, h).

#### NF- $\kappa$ B Signaling Is Downstream of the SPHK1 Function

Previous reports indicated SPHK1 activating the NF- $\kappa$ B signaling p65 in colon cancer.<sup>23</sup> Activating p65 stimulates proliferation of mammary epithelial cells.<sup>24</sup> So, we next examined whether the NF- $\kappa$ B signaling pathway was

activated in OSCC cells. SPHK1 knockdown decreased the expression of p65 and phosphoinositide-p65 (p-p65), which are key mediators of the NF- $\kappa$ B pathway in cells and tissues (Fig. 6a; Supplementary Fig. 4A). A pharmacologic approach using QNZ (Selleck Chemicals, TX) inhibited NF- $\kappa$ B activation. Administration of QNZ significantly inhibited proliferation, increased apoptosis, and decreased migration and invasion ability of Cal 27 cells, while shSPHK1 groups showed no significant difference after QNZ administration (Fig. 6b, g; Supplementary Fig. 4B, D).

In addition, we found that the expression of PP65 was upregulated after SPHK1 overexpression in HN6, suggesting activation of the NF- $\kappa$ B signaling pathway (Supplementary Fig. 3A). QNZ significantly inhibited the oncogenic phenotype induced by overexpression of SPHK1 (Supplementary Fig. 3B, F). These results indicate that p65 is a key QNZ downstream molecule, dominant in SPHK1 expression.

## DISCUSSION

During the progression of malignant tumors, metabolic enzymes change metabolic substrates and products, causing metabolic reprogramming of malignant tumors to meet the bioenergetic, biosynthetic, and redox demands of malignant cells.<sup>25</sup> Recently, metabolomics studies of malignant tumors have mainly focused on screening PCMs<sup>26</sup> and distinguishing tumor subtypes on the basis of metabolic characteristics. The role of metabolomics in PCMs research involves screening and verification. Large-scale screening through nontargeted high-throughput data fosters the preliminary discovery of PCMs and targeted quantitative verification of known PCMs. The high-resolution and high-sensitivity UPLC-MS technology<sup>27</sup> facilitates extensive screening and precise metabolite identification from highly mixed clinical samples, including plasma, serum, urine, saliva, and tissues.<sup>28</sup> Malignant tumors of the same anatomical origin contain different subtypes of individual or grouped gene mutations. Therefore, adopting the same treatment method has different efficacies between different subtypes. The LC-MS technology<sup>29</sup> distinguishes metabolic differences between tumor subtypes and traces upstream to explore potential therapeutic targets. Presently, metabolomics studies on oral squamous cell carcinoma tissues mainly involve NMR spectroscopy technology.<sup>30</sup> This study reports the first use of LC-MS technology to analyze the metabolic differences between oral squamous cell carcinoma tissues and adjacent tissues. Citrulline was the most significantly elevated non-exogenous metabolite in OSCC, but lysophosphatidylcholine, nonanoyl carnitine, homocitrulline, L-glutamine,



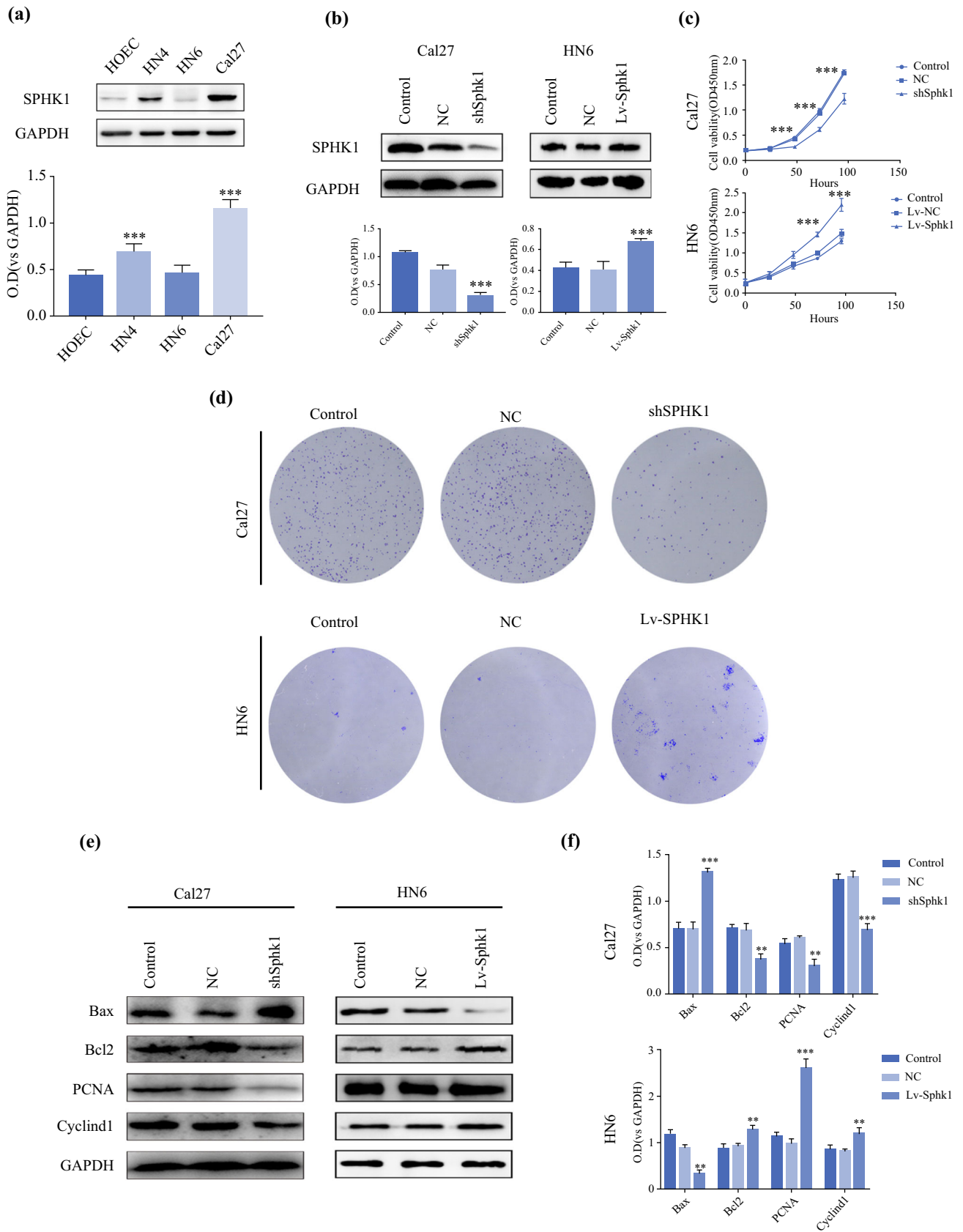


**FIG. 3** SPHK1 promoted cell proliferation and inhibited apoptosis in OSCC cells; **a** SPHK1 expression in human oral epithelial and oral carcinoma cell lines; **b** transfection efficiency measured by western blot in Cal 27 and HN6 cells; **c** proliferation ability of Cal 27 and HN6 cells measured by the CCK8 assay; **d** clone formation assay showing the clone formation ability of Cal27 and HN6 cells; **e**, **f** western blot expression and statistical results of apoptosis, proliferation, and cyclin-related proteins

metabolism, followed by arginine and proline, pyrimidine, glycerolipid, folate biosynthesis, D-glutamine and D-glutamate, glycine, serine and threonine, starch and sucrose, conversion of pentose and glucuronic acid, alanine, aspartic acid, and glutamate. Recent studies have shown that the sphingolipid metabolic pathway is associated with clinicopathological features and presented potential for the

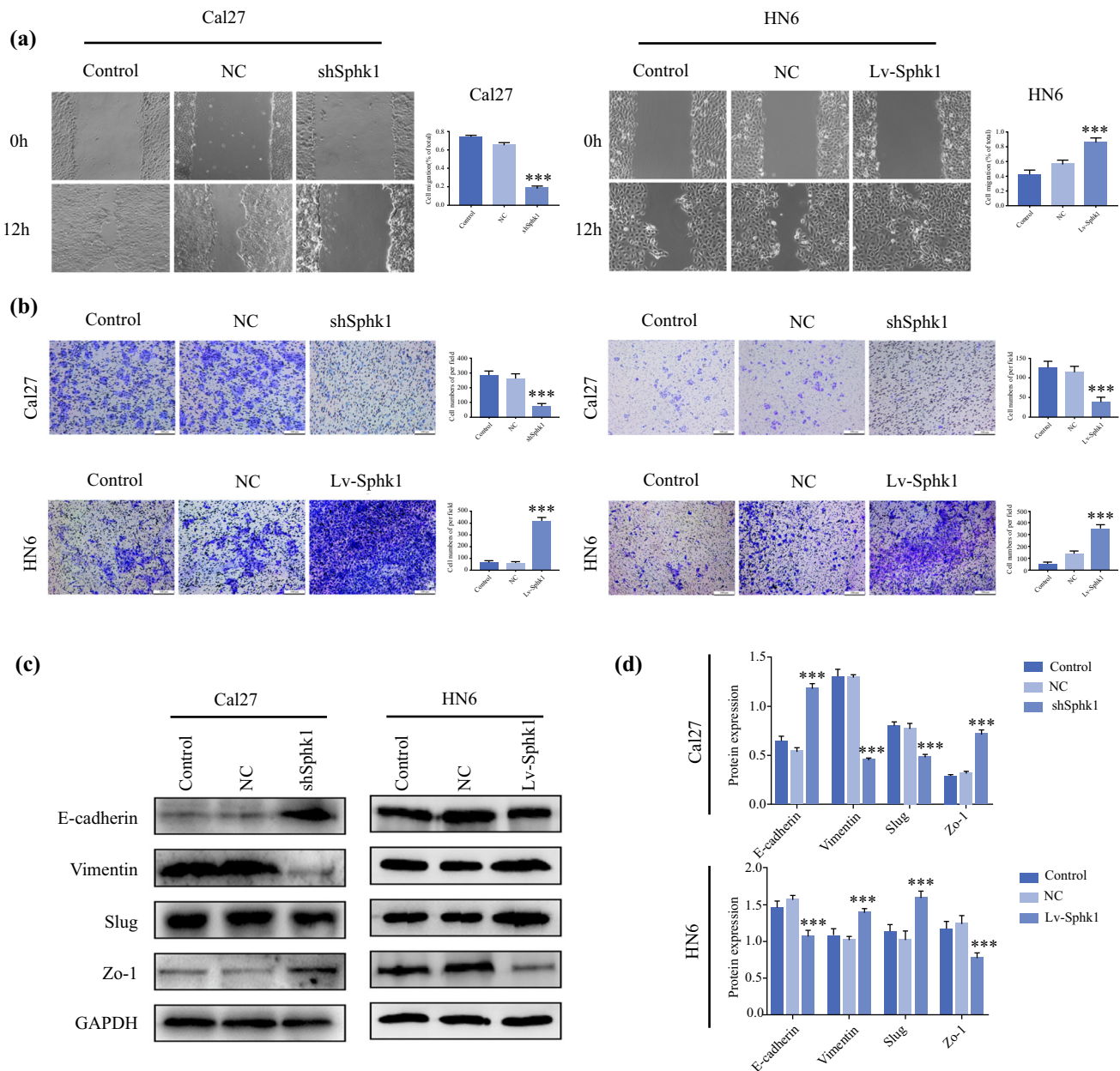


**FIG. 4** SPHK1 enhances epithelial-mesenchymal transformation (EMT) in OSCC cell lines; **a** the wound healing assay showing suppressed migration ability in Cal 27 and HN6 cells; **b** transwell

assays showing migration and invasion capacity in Cal 27 and HN6 cells; **c**, **d** western blot assay of EMT-associated protein expression

niacin, and creatine were considerably reduced. Sphingolipid was the most affected metabolic pathway

prediction of poor prognosis in OSCC patients, and the

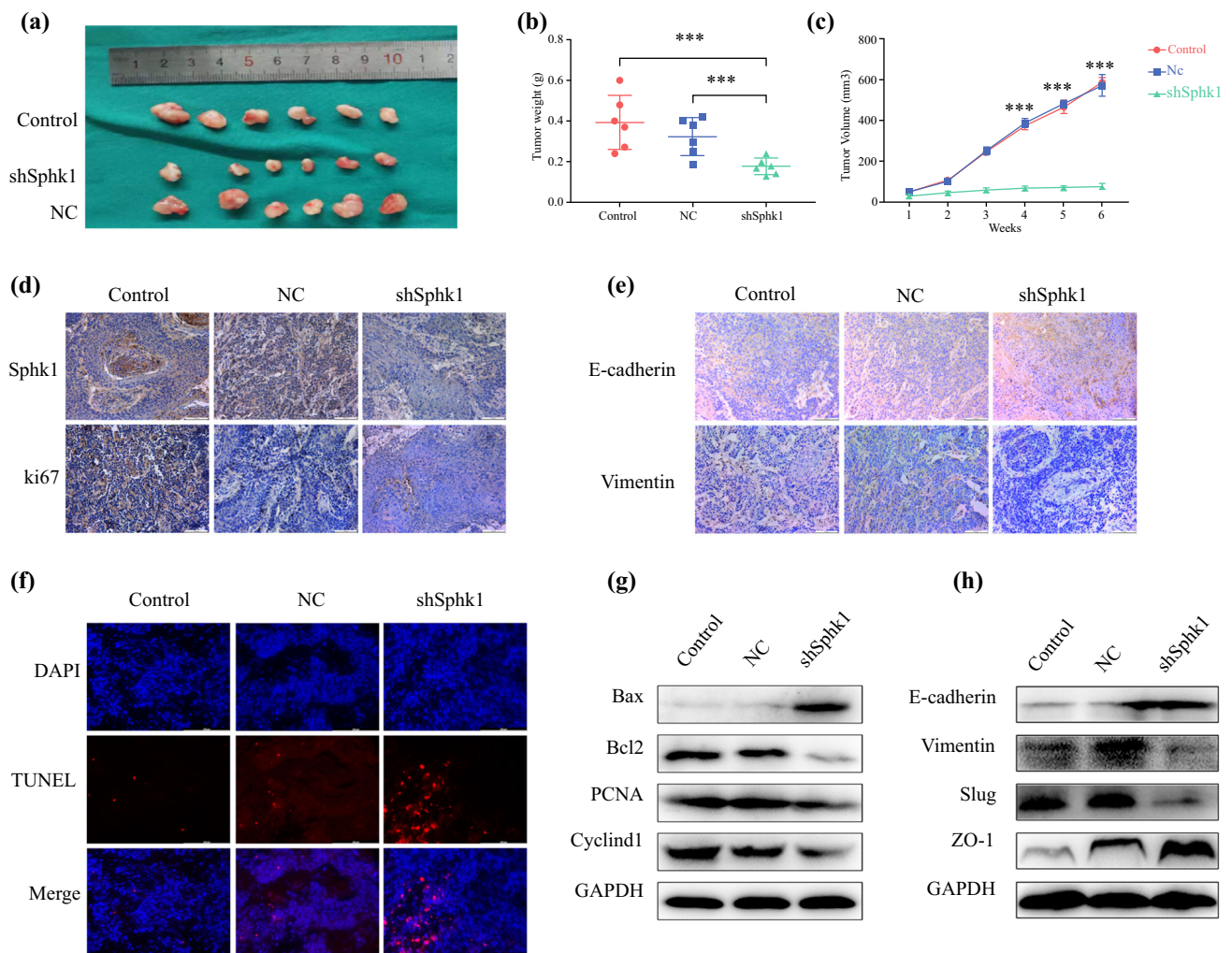


**FIG. 5** SPHK1 knockdown inhibits tumor growth; **a–c** Cal 27 cells with stably low SPHK1 expression (shSPHK1 groups) and control Cal 27 cells (NC groups) were inoculated into the left abdomen of nude mice to construct a xenograft tumor model of OSCC; photographs were taken 6 weeks after tumor transplantation; **d** immunohistochemistry analysis of SPHK1 and Ki67 expression in

SPHK1 knockdown and control groups; **e** immunohistochemical stains showing the expression of epithelial and stromal markers of transplanted tumors from Cal 27 cells with stable SPHK1 knockdown or controls; **f** TUNEL staining for apoptosis analysis of mouse xenograft specimens; **g, h** expression levels of proliferation, apoptosis, and EMT-related proteins in mouse xenograft specimens

sphingolipids signatures in plasma and tumor tissues as biomarker candidates for diagnosis and prognosis in OSCC.<sup>31</sup>

Sphingosine-1-phosphate, the sphingosine metabolite, promotes proliferation, inhibits apoptosis, and causes poor OSCC prognosis.<sup>32</sup> SPHK1, involved in sphingolipid metabolism, is a lipid kinase from a highly conserved family of lipid kinases. SPHK1 converts sphingosine to sphingosine-1-phosphate. SPHK1, located in the cytoplasm, is phosphorylated and activated in the cytoplasm, and transferred to the cell membrane, where it catalyzes sphingosine phosphorylation to produce sphingosine-1-phosphate, which it secretes outside the membrane. Sphingosine-1-phosphate binds to the receptor outside the cell membrane to promote tumor cell proliferation, migration,

and invasion.<sup>33</sup> SPHK1 is overexpressed in various malignant tumors and is highly correlated with poor prognosis. The role of SPHK1 in promoting tumor growth has been confirmed in gastric,<sup>34</sup> colorectal,<sup>35</sup> and breast cancer.<sup>36</sup> Recent studies have shown that SPHK1 promotes stem cell survival in breast cancer by inhibiting STAT1.<sup>37</sup> Although the potential oncogenic roles of SPHK1 in many varieties of cancer have been proved, its functions and mechanism remain vague and require further research.

The NF- $\kappa$ B/Rel family includes five proteins: p50, c-Rel, Rel-B, p52, and p65 (Rel-A) proteins, which form dimers to regulate gene expression by combining with  $\kappa$ B elements.<sup>38</sup> The NF- $\kappa$ B classical pathway activation triggers the release of p65 and p50 dimers from the inhibitory complex,<sup>39</sup> a function related to cell growth and survival.<sup>40</sup>



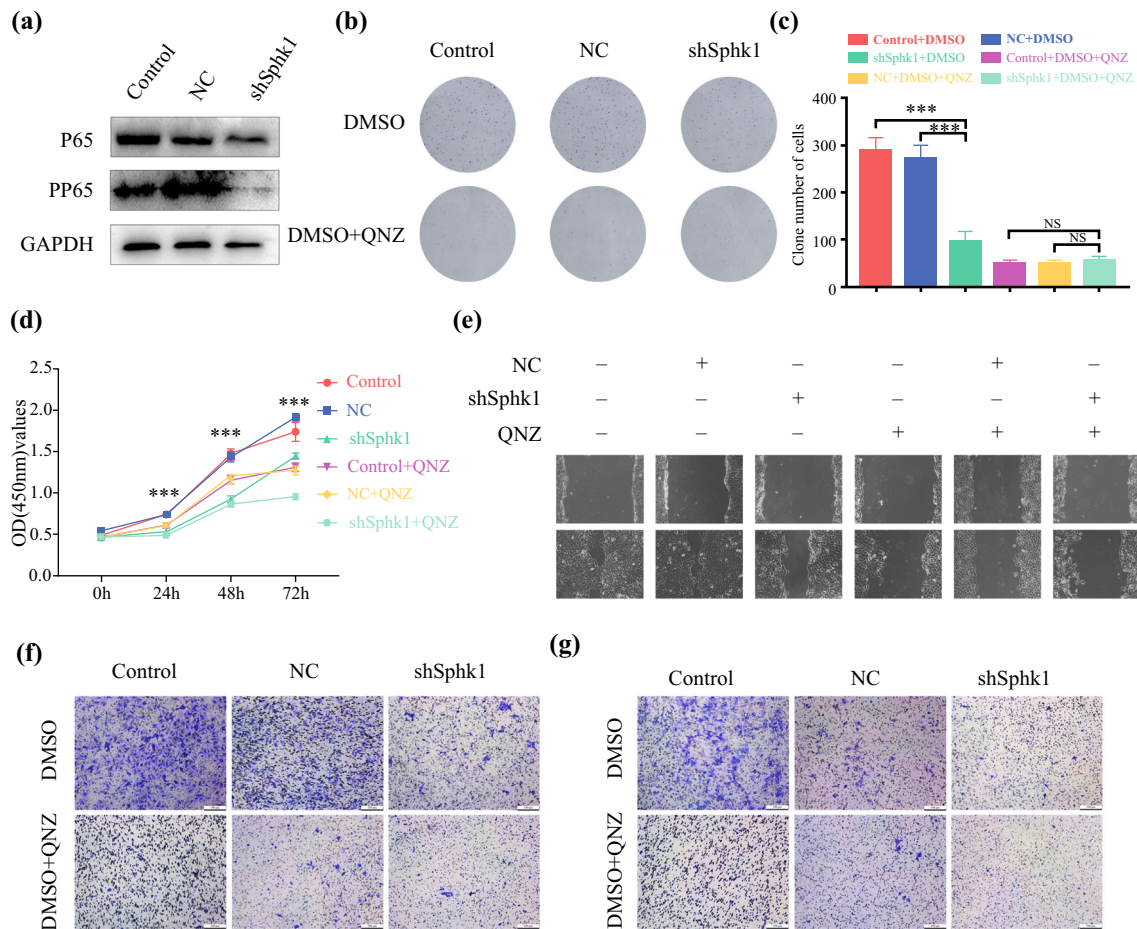


**FIG. 6** p65 is the main downstream of SPHK1 function; **a** western blot assay showing total and phosphorylated p65 levels in Cal 27 cells with stable SPHK1 knockdown or controls; **b–d** QNZ treatment

p65 reportedly regulates cell cycle, proliferation, and apoptosis in several cancers, and SPHK1 promotes p65 proliferation of mammary epithelial cells.<sup>41</sup> Therefore, this study hypothesized that SPHK, through p65, promotes the proliferation and migration of tumor cells and inhibits OSCC tumor cell apoptosis. SPHK1 positively correlates with the expression of p65 and the p65 active form (pp65) in cell and in vitro oncogenesis. Cal 27 cells treated with QNZ (a p65 inhibitor) showed the same response after SPHK1 knockdown, while the phenotype of Cal 27 cells treated with the QNZ showed no significant changes. Therefore, p65 is important downstream of SPHK1 in promoting tumor growth.

In conclusion, this study identified metabolic differences between OSCC and paired ANT, explored the carcinogenic role of overexpressed SPHK1, and revealed the association of SPHK1 with poor OSCC prognosis. SPHK1 targets NF- $\kappa$ B signaling by facilitating p65 expression to regulate

significantly reduced the proliferation ability of cells; **e–g** QNZ intervention significantly reduced the invasion and migration ability of cells

tumor progression and promote tumor metastasis, providing potential therapeutic targets for diagnosing and treating oral tumors.

**Supplementary Information** The online version contains supplementary material available at <https://doi.org/10.1245/s10434-022-12098-8>.

**ACKNOWLEDGEMENT** The authors thank Dr. Wei Zhang and Prof. Xiao-Ling Song for their excellent pathological technical support. This research was funded by the Priority Academic Program Development of Jiangsu Higher Education Institutions: PAPD, 2018-87; Jiangsu Provincial Medical Key Talent Project: ZDRCA2016087; Southeast University-Nanjing Medical University Cooperative Research Project: 2017DN03.

**AVAILABILITY OF DATA AND MATERIALS** All data generated or analyzed during this study are included in this published article.

**DISCLOSURE** All the authors listed above declare that they have no conflicts of interest.

**ETHICS APPROVAL** The study was approved by the Research Ethics Committee of Nanjing Medical University, China.

**PATIENT CONSENT** Informed consent was obtained from the patients.

## REFERENCES

- Bloebaum M, Poort L, Böckmann R, et al. Survival after curative surgical treatment for primary oral squamous cell carcinoma. *J Craniomaxillofac Surg.* 2014;42(8):1572–6.
- Gangopadhyay A, Bhatt S, Nandy K, et al. Survival impact of surgical resection in locally advanced T4b oral squamous cell carcinoma. *Laryngoscope.* 2021;131(7):E2266–74.
- Flörke C, Gülses A, Altmann CR, et al. Clinicopathological risk factors for contralateral lymph node metastases in intraoral squamous cell carcinoma: a study of 331 cases. *Curr Oncol.* 2021;28(3):1886–98.
- Panarese I, Aquino G, Ronchi A, et al. Oral and oropharyngeal squamous cell carcinoma: prognostic and predictive parameters in the etiopathogenetic route. *Expert Rev Anticancer Ther.* 2019;19(2):105–19.
- Wolff KD, Follmann M, Nast A. The diagnosis and treatment of oral cavity cancer. *Dtsch Arztebl Int.* 2012;109(48):829–35.
- Almangush A, Mäkitie AA, Triantafyllou A, et al. Staging and grading of oral squamous cell carcinoma: An update. *Oral Oncol.* 2020;107:104799.
- Vitório JG, Duarte-Andrade FF, Dos Santos Fontes Pereira T, et al. Metabolic landscape of oral squamous cell carcinoma. *Metabolomics.* 2020;16(10):105.
- Wang L, Wang X, Li Y, et al. Plasma lipid profiling and diagnostic biomarkers for oral squamous cell carcinoma. *Oncotarget.* 2017;8(54):92324–32.
- Yonezawa K, Nishiumi S, Kitamoto-Matsuda J, et al. Serum and tissue metabolomics of head and neck. *Cancer Genomics Proteomics.* 2013;10(5):233–8.
- Tsai CK, Lin CY, Kang CJ, et al. Nuclear magnetic resonance metabolomics biomarkers for identifying high risk patients with extranodal extension in oral squamous cell carcinoma. *J Clin Med.* 2020;9(4):951.
- Wei J, Xie G, Zhou Z, et al. Salivary metabolite signatures of oral cancer and leukoplakia. *Int J Cancer.* 2011;129(9):2207–17.
- Mikkonen JJ, Singh SP, Herrala M, et al. Salivary metabolomics in the diagnosis of oral cancer and periodontal diseases. *J Periodontol Res.* 2016;51(4):431–7.
- Somashekar BS, Kamarajan P, Danciu T, et al. Magic angle spinning NMR-based metabolic profiling of head and neck squamous cell carcinoma tissues. *J Proteome Res.* 2011;10(11):5232–41.
- Zheng X, Li W, Ren L, et al. The sphingosine kinase-1/sphingosine-1-phosphate axis in cancer: potential target for anticancer therapy. *Pharmacol Ther.* 2019;195:85–99.
- Wollny T, Watek M, Durnas B, et al. Sphingosine-1-phosphate metabolism and its role in the development of inflammatory bowel disease. *Int J Mol Sci.* 2017;18(4):741.
- Dai L, Wang W, Liu Y, et al. Inhibition of sphingosine kinase 2 down-regulates ERK/c-Myc pathway and reduces cell proliferation in human epithelial ovarian cancer. *Ann Transl Med.* 2021;9(8):645.
- Song L, Xiong H, Li J, et al. Sphingosine kinase-1 enhances resistance to apoptosis through activation of PI3K/Akt/NF- $\kappa$ B pathway in human non-small cell lung cancer. *Clin Cancer Res.* 2011;17(7):1839–49.
- Shida D, Fang X, Kordula T, et al. Cross-talk between LPA1 and epidermal growth factor receptors mediates up-regulation of sphingosine kinase 1 to promote gastric cancer cell motility and invasion. *Cancer Res.* 2008;68(16):6569–77.
- Grbcic P, Tomljanovic I, Klobucar M, et al. Dual sphingosine kinase inhibitor SKI-II enhances sensitivity to 5-fluorouracil in hepatocellular carcinoma cells via suppression of osteopontin and FAK/IGF-1R signalling. *Biochem Biophys Res Commun.* 2017;487(4):782–8.
- Uranbileg B, Ikeda H, Kurano M, et al. Increased mRNA levels of sphingosine kinases and s1p lyase and reduced levels of s1p were observed in hepatocellular carcinoma in association with poorer differentiation and earlier recurrence. *PLoS One.* 2016;11(2):e0149462.
- Acharya S, Yao J, Li P, et al. Sphingosine kinase 1 signaling promotes metastasis of triple-negative breast cancer. *Cancer Res.* 2019;79(16):4211–26.
- Bao Y, Guo Y, Zhang C, et al. Sphingosine kinase 1 and sphingosine-1-phosphate signaling in colorectal cancer. *Int J Mol Sci.* 2017;18(10):2109.
- Shen Z, Feng X, Fang Y, et al. POTEE drives colorectal cancer development via regulating SPHK1/p65 signaling. *Cell Death Dis.* 2019;10(11):863.
- Li S, Zheng X, Wu X, et al. Sphk1 promotes breast epithelial cell proliferation via NF- $\kappa$ B-p65-mediated cyclin D1 expression. *Oncotarget.* 2016;6(49):80579–85.
- DeBerardinis RJ, Chandel NS. Fundamentals of cancer metabolism. *Sci Adv.* 2016;2(5):e1600200.
- Xiao Q, Zhang F, Xu L, et al. High-throughput proteomics and AI for cancer biomarker discovery. *Adv Drug Deliv Rev.* 2021;176:113844.
- Nassar AF, Wu T, Nassar SF, et al. UPLC-MS for metabolomics: a giant step forward in support of pharmaceutical research. *Drug Discov Today.* 2017;22(2):463–70.
- Xie F, Liu T, Qian WJ, et al. Liquid chromatography-mass spectrometry-based quantitative proteomics. *J Biol Chem.* 2011;286(29):25443–9.
- Chaleckis R, Meister I, Zhang P, Wheelock CE. Challenges, progress and promises of metabolite annotation for LC-MS-based metabolomics. *Current Opin Biotechnol.* 2019;55:44–50.
- Duarte D, Castro B, Pereira JL, et al. Evaluation of saliva stability for NMR metabolomics: collection and handling protocols. *Metabolites.* 2020;10(12):515.
- Faedo RR, Ushida TR, Lacchini R, et al. Sphingolipids signature in plasma and tissue as diagnostic and prognostic tools in oral squamous cell carcinoma. *Biochim Biophys Acta Mol Cell Biol Lipids.* 2022;1867(1):159057.
- Kato K, Shimasaki M, Kato T, et al. Expression of sphingosine kinase-1 is associated with invasiveness and poor prognosis of oral squamous cell carcinoma. *Anticancer Res.* 2018;38(3):1361–8.
- Gomez-Larrauri A, Presa N, Dominguez-Herrera A, et al. Role of bioactive sphingolipids in physiology and pathology. *Essays Biochem.* 2020;64(3):579–89.
- Sukocheva OA, Furuya H, Friedemann M, et al. Sphingosine kinase and sphingosine-1-phosphate receptor signaling pathway in inflammatory gastrointestinal disease and cancers: a novel therapeutic target. *Pharmacol Ther.* 2020;207:107464.
- Xu C, Zhang W, Liu S, et al. Activation of the SphK1/ERK/p-ERK pathway promotes autophagy in colon cancer cells. *Oncol Lett.* 2018;15(6):9719–24.
- Imbert C, Montfort A, Fraisse M, et al. Resistance of melanoma to immune checkpoint inhibitors is overcome by targeting the sphingosine kinase-1. *Nat Commun.* 2020;11(1):437.
- Hii LW, Chung FF, Mai CW, et al. Sphingosine kinase 1 regulates the survival of breast cancer stem cells and non-stem breast cancer cells by suppression of STAT1. *Cells.* 2020;9(4):886.



38. Giridharan S, Srinivasan M. Mechanisms of NF-kappaB p65 and strategies for therapeutic manipulation. *J Inflamm Res.* 2018;11:407–19.
39. Amaro-Leal Â, Shvachiy L, Pinto R, et al. Therapeutic effects of Ikb kinase inhibitor during systemic inflammation. *Int Immunopharmacol.* 2020;84:106509.
40. Wang Y, Xu H, Jiao H, et al. STX2 promotes colorectal cancer metastasis through a positive feedback loop that activates the NF-kappaB pathway. *Cell Death Dis.* 2018;9(6):664.
41. Schmitz ML, Kracht M. Cyclin-dependent kinases as coregulators of inflammatory gene expression. *Trends Pharmacol Sci.* 2016;37(2):101–13.

**Publisher's Note** Springer Nature remains neutral with regard to jurisdictional claims in published maps and institutional affiliations.